ADVANCES IN ATMOSPHERIC SCIENCES, VOL. 31, JANUARY 2014, 154–164

Impacts of Four Types of ENSO Events on Tropical Cyclones Making Landfall over Mainland China Based on Three Best-track Datasets

ZHANG Han[1,2] and GUAN Yuping*[1]

[1]*State Key Laboratory of Tropical Oceanography, South China Sea Institute of Oceanology, Chinese Academy of Sciences, Guangzhou* 510301

[2]*Graduate University of Chinese Academy of Sciences, Beijing* 100039

(Received 10 July 2012; revised 29 March 2013; accepted 15 April 2013)

ABSTRACT

Impacts of El Niño Modoki (ENM), La Niña Modoki (LNM), canonical El Niño (CEN) and canonical La Niña (CLN) on tropical cyclones (TCs) that made landfall over mainland China during 1951–2011 are analysed using best-track data from China, the USA and Japan. Relative to cold phase years (LNM and CLN), landfalling TCs in warm years (ENM and CEN) have a farther east genesis location, as well as longer track lengths and durations, both in total and before landfall. ENM demonstrates the highest landfall frequency, most northerly mean landfall position, and shortest after-landfall sustainability (track length and duration), which indicate a more frequent and extensive coverage of mainland China by TCs, but with shorter after-landfall influence. CEN has low landfall frequency and the most southerly mean landfall location. LNM has the most westerly genesis location, being significantly farther west than the 1951–2011 average and leading to short mean track lengths and durations both in total or before landfall, all of which are significantly shorter than the 1951–2011 average. Variations in the low-level wind anomaly, vertical wind shear, mid-level relative humidity, steering flow, the monsoon trough and the western Pacific subtropical high (WPSH) can to some extent account for the features of frequency, location, track length and duration of landfalling TCs. Since ENSO Modoki is expected to become more frequent in the near future, the results for ENSO Modoki presented in this paper are of particular significance.

Key words: El Niño–Southern Oscillation, tropical Pacific anomaly, tropical storm, coastal China, thermodynamic and dynamic analysis

Citation: Zhang, H., and Y. P. Guan, 2014: Impacts of four types of ENSO events on tropical cyclones making landfall over mainland China based on three best-track datasets. *Adv. Atmos. Sci*., **31**(1), 154–164, doi: 10.1007/s00376-013-2146-8.

1. Introduction

The El Niño–Southern Oscillation (ENSO) is the strongest signal in the tropical Pacific. Different ENSO phases associated with different large-scale circulation and environmental conditions affect tropical cyclone (TC) frequency, genesis location and trajectory (Chia and Ropelewski, 2002; Wang and Chan, 2002). TCs tend to extend farther southeast (northwest) during El Niño (La Niña) years (Elsner and Liu, 2003; Camargo et al., 2007). Relative to neutral years, TC landfall frequency in the late season of El Niño years over the landmasses surrounding the western North Pacific (WNP) is significantly reduced, except over Japan and the Korean Peninsula, and more (fewer) TCs tend to make landfall over China during years associated with La Niña (El Niño) events (Liu and Chan, 2003; Wu et al., 2004). However, recent studies (Ashok et al., 2007; Yeh et al., 2009) have shown that El Niño Modoki (sea surface warming in the central Pacific near the dateline) is a different SST phase from that occurring in canonical El Niño (abnormal warming in the eastern Pacific); the latter has been less frequent and the former is becoming more common. Some studies refer to ENSO Modoki as the "central Pacific ENSO" (Kao and Yu, 2009) or "Warm-Pool ENSO" (Kug et al., 2009). Recent studies on TCs have started to distinguish between these different types of ENSO events. TC frequency is significantly positively correlated with the ENSO Modoki index (EMI) (Chen and Tam, 2010): above-normal (below-normal) TC frequency over the South China Sea occurs during June–August (September–November) in El Niño Modoki years (canonical El Niño years) (Chen, 2011). Kim et al. (2011) showed that, compared with canonical El Niño years, the TC activity in El Niño Modoki years is shifted to the west and extends through the northwestern part of the western Pacific. Hong et al. (2011) showed a small difference in TC tracks between El Niño Modoki and canonical El Niño in boreal summer (June–August), but in boreal autumn (September–November) TCs recurve northward at farther westward locations near the coastline of East Asia during El Niño Modoki

* Corresponding author: GUAN Yuping
E-mail: guan@scsio.ac.cn

years. Zhang et al. (2012) demonstrated that TCs have a greater probability of making landfall over Japan and Korea during both summer and the whole June–October (JJASO) period for El Niño Modoki years, while in autumn of these years, TC landfall in most areas of East Asia is likely to be suppressed.

More TCs make landfall over China than in most other countries. Although several studies have examined the impact of ENSO events on TCs that make landfall over China (e.g., Liu and Chan, 2003; Fogarty et al., 2006; Wang and Song, 2009), recent research on ENSO Modoki suggests that the effect of ENSO on landfalling TCs over China needs to be revisited. There have been several studies of TCs in the WNP and East Asia that distinguish between canonical ENSO and ENSO Modoki, including TCs affecting China (Chen and Tam, 2010; Chen, 2011; Hong et al., 2011; Kim et al., 2011; Zhang et al., 2012), but their results for TCs landfalling over China are rough and disparate. Moreover, most of these studies were focused on just two or three ENSO patterns (El Niño Modoki and canonical El Niño, or additionally canonical La Niña) and used only one TC dataset. Thus, in this context, the present paper attempts to investigate in detail the characteristics of TCs that make landfall over China in all four patterns of ENSO (El Niño Modoki, canonical El Niño, La Niña Modoki and canonical La Niña). Since TCs making landfall over mainland China, Taiwan and Hainan Island have different characteristics (Ren et al., 2008; Wang et al., 2012; Zhang and Guan, 2012a, 2012b), we only consider TCs over mainland China. In addition, because TC frequency and location differ in different datasets (Liang et al., 2010; Ren et al., 2011), we selected three best-track datasets from China, the USA and Japan, and focus on common phenomena among the three datasets. In brief, the present paper analyses the impact of four patterns of ENSO on landfalling TCs using three best-track datasets from China, the USA and Japan. We hope this work will help to improve understanding of the influence of ENSO on TCs that make landfall over China.

2. Data and method

The three TC best-track datasets used in this study were obtained from: (i) the China Meteorological Administration (CMA, http://www.typhoon.gov.cn); (ii) the Joint Typhoon Warning Centre (JTWC, http://weather.unisys.com/hurricane/w_pacific/); and (iii) the Japanese Meteorological Agency (JMA, http://www.jma.go.jp/jma/jma-eng/jma-center/rsmc-hp-pub-eg/besttrack.html). In addition, the EMI and Niño3 index were used to identify ENSO Modoki and canonical ENSO. The EMI data were obtained from the Japan Agency for Marine-Earth Science and Technology (JAMSTEC, http://www.jamstec.go.jp/frcgc/research/d1/iod/modoki_home.html.en), and the Niño3 index data from the Koninklijk Nederlands Meteorologisch Instituut (KNMI, http://climexp.knmi.nl/). Atmospheric data were obtained from the National Centers for Environmental Prediction–National Center for Atmospheric Research (NCEP–NCAR) Reanalysis (Kalnay et al., 1996), while SST data were from the Hadley Centre SST (HadISST) dataset (Rayner et al., 2003).

The three best-track datasets cover the periods 1949–2011 (CMA), 1945–2011 (JTWC), and 1951–2011 (JMA), and thus the comparisons and analyses presented in this paper are based on all the data from the period 1951–2011. Note that only TCs with the intensity of a tropical storm or higher ($\geqslant 17.2$ m s^{-1}) are considered because of the possible large errors in counting tropical depressions. Similarly, genesis location is defined as the position when the intensity of a cyclone is first equal to or greater than a tropical storm. Landfall locations are defined as the intersections of TC tracks and coastline; if a single TC has more than one landfall point, we only count the first one. We mainly use the CMA data, as this dataset has been shown to be more complete and to have more accurate information for TCs that affect China (Liang et al., 2010; Ren et al., 2011). We use the other two best-track datasets as supporting data. In the three datasets, the majority of TCs make landfall over mainland China during June to October (JJASO): CMA, 94.9%; JTWC, 95.1%; JMA, 95.8%. We therefore use JJASO mean EMI and Niño3 indices for analysis unless otherwise indicated. After removing the linear trend of JJASO average EMI, El Niño Modoki (ENM) years were defined as those for which JJASO average EMI was greater than one standard deviation, and La Niña Modoki (LNM) years for which it was below one negative standard deviation. In order of decreasing strength, the years for ENM were thus defined to be: 1994, 2004, 1966, 2002, 1991, 1977 and 1967; and for LNM they were 1983, 1998, 1975, 2010, 1988, 2008, 1999, 1974, 1973 and 1956. By the same method we defined canonical El Niño (CEN) years (1997, 1972, 1987, 1982, 1965, 1976, 1957, 2009, 1963 and 1951) and canonical La Niña (CLN) years (1988, 1970, 1973, 2010, 2007, 1999, 1964, 1955, 1954 and 1975). Research has demonstrated the existence of LNM (Ashok et al., 2007; Kao and Yu, 2009), but it is difficult to separate LNM from CLN because of their similarity in SST patterns, and the independence of LNM from CLN is weaker than between warm events (Kug et al., 2009; Kug and Ham, 2011). In the present paper, although LNM and CLN were found to have five overlapping years (2010, 1988, 1975, 1999 and 1973), we still study them separately below.

3. Landfalling tropical cyclones and ENSO

3.1. *Overview*

In the three datasets, 5.0–5.4 TCs make landfall over mainland China every year, which is approximately about 19.5%, 19.3% and 20.8% (CMA, JTWC and JMA, respectively) of the TCs in the Western North Pacific (WNP) during 1951–2011 (Table 1). Average landfall latitude is about 24.22°–24.46°N, which is on the coastline of Fujian Province, China. Meanwhile, landfall wind speed is about half of the maximum wind speed of all landfalling TCs. Table 2 shows that before-landfall track length and duration are longer than after-landfall equivalents, and TCs seem to travel

Table 1. Frequency, location and wind of landfalling TCs over mainland China during 1951–2011. "Genesis frequency" and "Landfall frequency" are respectively the total generated frequency in the WNP and landfall frequency over mainland China, with annual averages shown in brackets. Landfall wind speed was taken to be the wind speed of the data point that was nearest to the coastline before landfall. Values in other columns are averages of all landfalling TCs. Wind data from JMA were not included because wind speed was not recorded before 1977.

	Landfall frequency	Genesis frequency	Landfall latitude (°E)	Genesis latitude (°E)	Genesis longitude (°E)	Landfall wind speed ($m\ s^{-1}$)	Max wind speed ($m\ s^{-1}$)
CMA	325 (5.3)	1668 (27.3)	24.46	17.68	127.95	23.59	44.02
JTWC	306 (5.0)	1583 (26.0)	24.22	16.48	130.41	24.73	46.45
JMA	331 (5.4)	1594 (26.1)	24.27	16.71	129.20	-	-

Table 2. Average sustainability (track length, duration) and destructive ability (PDI) of landfalling TCs over mainland China during 1951–2011. "After" and "Before" mean "after landfall" and "before landfall". PDI in JMA was not included because no wind speed data were recorded before 1977.

	Track length (m)			Duration (h)			PDI (10^5)		
	After	Before	Total	After	Before	Total	After	Before	Total
CMA	1238.3	1610.2	2848.5	47.8	96.5	144.3	0.81	11.6	12.4
JTWC	751.2	1950.1	2710.7	27.9	154.5	182.5	0.91	14.4	15.3
JMA	1553.3	1853.1	3406.4	58.3	114.8	173.1	-	-	-

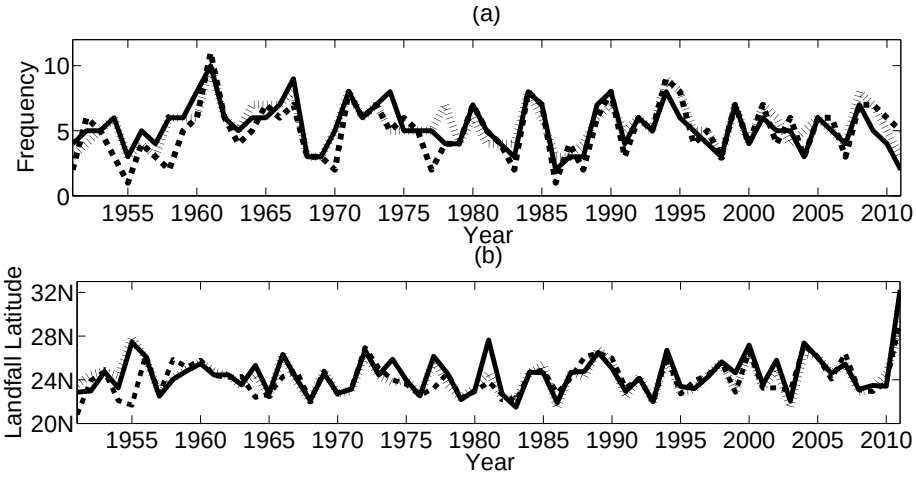

Fig. 1. Landfall (a) frequency and (b) latitude of landfalling TCs over mainland China based on CMA (solid line), JTWC (dashed line) and JMA (dotted line) data.

faster after landfall because the percentage of after-landfall track length with respect to the total is greater than that of after-landfall duration. JTWC shows shorter after-landfall track length and duration than CMA and JMA. After-landfall Potential Destructive Index (PDI, Emanuel, 2005) is much smaller than before-landfall PDI. Annual frequency and landfall latitude are also shown in Fig. 1. For further detail on the variability and distribution of TCs that make landfall over mainland China, see Zhang and Guan (2012b).

3.2. *Time series correlation*

To gain at least a rough understanding of the impact of ENSO Modoki and canonical ENSO, this section covers the correlation between EMI (Niño3) and characteristic quantities of landfalling TCs given in Tables 1 and 2. Note that all the characteristic quantities we discuss here, including genesis location (but not genesis frequency), are average values of landfalling TCs.

The results show that EMI has a good relationship with TC genesis frequency in the WNP, with correlation coefficients of 0.382**, 0.294* and 0.346** in CMA, JTWC and JMA data (hereafter, groups of three values always refer to the three datasets in order, with "*" meaning above the 95% confidence level and "**" meaning above 99%). The correlation between Niño3 and landfall latitude (genesis latitude) is significant in all three datasets, with correlation coefficients of -0.360**, -0.410** and -0.355** (-0.377**, -0.355** and -0.361**), respectively. As TC locations and intensity often differ in the three datasets because of different observational techniques (Liang et al., 2010; Ren et al., 2011), we also show relationships that are significant in two datasets here: EMI and total duration, which have correlation coefficients of 0.270*, 0.134 and 0.264*. Meanwhile, Niño3 and total duration (before-landfall) have correlation coeffi-

cients of 0.253*, 0.392** and 0.184 (0.300**, 0.351** and 0.217). The correlation between Niño3 and before-landfall track length is also significant (0.271*, 0.297* and 0.201).

In conclusion, during 1951–2011, higher Niño3 or EMI generally corresponds with greater TC sustainability (track length, duration), but has little significant impact on landfall frequency or TC strength (wind speed, PDI).

As the ENSO effect in moderate years may be masked by other tropical signals, we analyse only the strong ENSO years in the next section, i.e., ENM, LNM, CEN and CLN years.

4. The four types of ENSO events

4.1. *Overview*

Tables 3 and 4 show annual-mean characteristic quantities of landfalling TCs in each type of ENSO event, and Figs. 2 and 3 show genesis locations, landfall locations and TC tracks in CMA data. These characteristics, which show consistent behaviour across the three datasets, are analysed here. Note that all the characteristic quantities we discuss here are average values of landfalling TCs, including genesis location (but not genesis frequency). The two-tailed Student's *t*-test was used to check the deviation of each quantity from the mean, and a Least Significant Difference (LSD) method (Fisher, 1935; Miller, 1966, p. 90) was used to compare the differences between pairs of different ENSO events. We also calculated the results for the five and seven strongest years of each type of ENSO event (not shown) and found conclusions very similar to the results presented in this section.

4.2. *Frequency*

Annual landfall (genesis) frequency directly reflects whether an ENSO event favors TC landfall (generation). In ENM years, the annual number of TCs that hit mainland China or form in the WNP is greater than during other types of ENSO events in the three datasets (Table 3), while LNM years have the least genesis frequency.

Table 3. Average frequency, location and wind in different types of landfalling TCs over mainland China in different types of ENSO events during 1951–2011. Apart from "Genesis frequency", all quantities are mean values of TCs that made landfall over mainland China. Bold values are maxima of each characteristic quantity in each dataset, while underlined values are minimums. "*" and "**" mean the quantity deviates from the mean value above the 95% and 99% confidence levels respectively, according to the two-tailed *t*-test.

	Landfall frequency	Genesis frequency	Landfall latitude (°N)	Genesis latitude (°N)	Genesis longitude (°E)	Landfall wind speed ($m\ s^{-1}$)	Max wind speed ($m\ s^{-1}$)
CMA-ENM	**5.9**	**31.9**	**25.57**	**18.81**	**129.75**	22.27	43.00
CMA-LNM	5.2	23.1	24.47	18.74	124.10**	**24.48**	39.50*
CMA-CEN	4.6	25.9	23.64	16.61	127.34	24.00	44.04
CMA-CLN	5.0	25.2	24.42	17.76	126.11	22.46	**46.12**
JTWC-ENM	**4.9**	**28.9**	**24.88**	**18.83****	129.00	**25.66**	43.88
JTWC-LNM	**4.9**	22.2	24.06	17.34	126.78*	24.04	44.57
JTWC-CEN	4.7	25.8	23.62	15.31	**130.11**	21.45**	44.35
JTWC-CLN	4.2	23.2	23.72	16.71	127.50	25.17	**49.91**
JMA-ENM	**6.4**	**30.6**	**25.17**	**18.26***	**128.92**	-	-
JMA-LNM	5.2	22.5	23.90	17.15	126.22*	-	-
JMA-CEN	4.8	25.4	23.59	15.75	128.31	-	-
JMA-CLN	5.3	24.2	24.29	16.61	127.58	-	-

Table 4. Average sustainability (track length, duration) and destructive ability (PDI) of landfalling TCs over mainland China in different types of ENSO events during 1951–2011. All the annotations are the same as in Table 2 and 3.

	Track length (m)			Duration (h)			PDI (10^5)		
	After	Before	Total	After	Before	Total	After	Before	Total
CMA-ENM	1076.8	**1786.3**	2863.1	40.0*	**107.8**	147.8	0.71	10.4	11.1*
CMA-LNM	1147.0	1171.9**	2318.9**	44.2	74.5**	118.7**	**0.86**	7.2**	8.0**
CMA-CEN	**1190.4**	1688.5	**2878.9**	**51.1**	107.7	**158.9**	0.80	12.8	13.6
CMA-CLN	1237.2	1462.9	2700.1	48.7	88.0	136.7	0.72	**14.0**	**14.7**
JTWC-ENM	636.0	1696.4	2332.4	21.2**	153.2	174.4	**1.02**	12.7	13.7
JTWC-LNM	757.6	1621.3	2378.8	31.6	136.3*	167.9	0.80	10.8	11.6
JTWC-CEN	**775.4**	**2064.8**	**2840.2**	**35.4**	**159.3**	**194.7**	0.62**	14.8	15.4
JTWC-CLN	694.1	1698.3	2392.4	26.0	135.6*	161.6*	0.77	**16.1**	**16.9**
JMA-ENM	1372.2	1832.8	3205.0	53.1	**123.2**	176.3	-	-	-
JMA-LNM	1270.7	1524.1*	2794.8**	48.9	93.9**	142.8**	-	-	-
JMA-CEN	**1539.8**	**1839.5**	**3379.4**	**63.5**	116.5	**180.0**	-	-	-
JMA-CLN	1455.0	1732.1	3187.1	54.1	104.4	158.5	-	-	-

4.3. *Location*

TC landfall location is probably the most important characteristic for both decision-makers and the wider population, and genesis location reflects to some extent the modulation effect of each ENSO event. Here, we examine the zonal and meridional characteristics of landfall and genesis location. Because landfall latitude generally determines landfall longitude on the coastline of mainland China, it is not necessary to discuss zonal landafall.

Table 3 shows that TCs in ENM make landfall (are generated) at higher latitudes than for the other three types of ENSO events, and have landfall (genesis) latitudes of about 0.7°–1.1° (1.1°–2.3°) farther north than the average (Table 1), while CEN shows landfall (genesis) latitudes lower than average. LSD results show that there may be a difference between landfall latitude between CEN and ENM, with statistical significance (p) values of 0.030*, 0.096 and 0.050*; while genesis latitude between CEN and ENM, CEN and LNM may also be significant (p values are 0.015*, 0.001**, 0.002** and 0.013*, 0.015*, 0.068 in CMA, JTWC and JMA data, respectively). The genesis longitude of landfalling TCs in warm events (ENM and CEN) lies to the east of that for cold events (LNM and CLN), while genesis longitude in LNM is significantly lower than average. Note that genesis longitude in LNM is significantly west of the mean.

There is some evidence for these features in Fig. 2. The genesis points in ENM are relatively scattered, spreading to the northeast, while genesis points in LNM tend to cluster in the west. The distribution of landfall frequency with latitude in each ENSO phase is shown in the histograms with unit latitude bins in Fig. 2. These show firstly that TCs tend to make landfall south of 30°N. Only six, three, one and five (14.6%, 5.6%, 2.1% and 9.8% of all landfalling TCs in each type) TCs make landfall north of 30°N in ENM, LNM, CEN and CLN, respectively. Second, landfall numbers in 21°–23°N are more than in other bands, with about 30.1%, 46.1%, 45.7% and 52.0% of TCs making landfall in ENM, LNM, CEN and CLN, respectively. Third, a greater percentage of TCs in ENM tend to make landfall along the northern coast of mainland China, while TCs in CLN tend to make landfall south of 25°N. Fourth, as Zhang and Guan (2012b) showed, 23°–24°N is an abnormal interval, with landfall frequency being smaller than over adjacent areas, although landfall frequency during 1951–2011 decreases from south to north. This feature is also found during all four types of ENSO events.

4.4. *Track and duration*

The track determines the area affected by a TC. Although it is difficult to find a clear difference in the other three ENSO events in Fig. 3, TC tracks in CEN years are constrained to a narrow region tilted from northwest to southeast. This is the monsoon trough region, and TCs in CEN tend to generate in this region (Fig. 2). TC tracks in CEN are also straighter than in the other three ENSO events.

Track length and duration represent the sustainability of a TC, and can themselves be further divided into three specific aspects: after-landfall, before-landfall, and total (Table 4). After-landfall features are more important because they directly relate to the impact of a landfalling TC. It is worth noting that mean values of after-landfall track length and duration in JMA are significantly greater than in CMA, and then CMA averages are greater than in JTWC. Track length and duration in CEN (LNM) seem the longest (shortest) in the four types of ENSO events. It is interesting that, although before-landfall and total track length and duration in warm years (ENM and CEN) are longer than in cold years (LNM and CEN), ENM has the shortest after-landfall sustainability (track length and duration). LSD results show that before-landfall duration between ENM and LNM may differ significantly, with p values of 0.013*, 0.302 and 0.047*. Note that

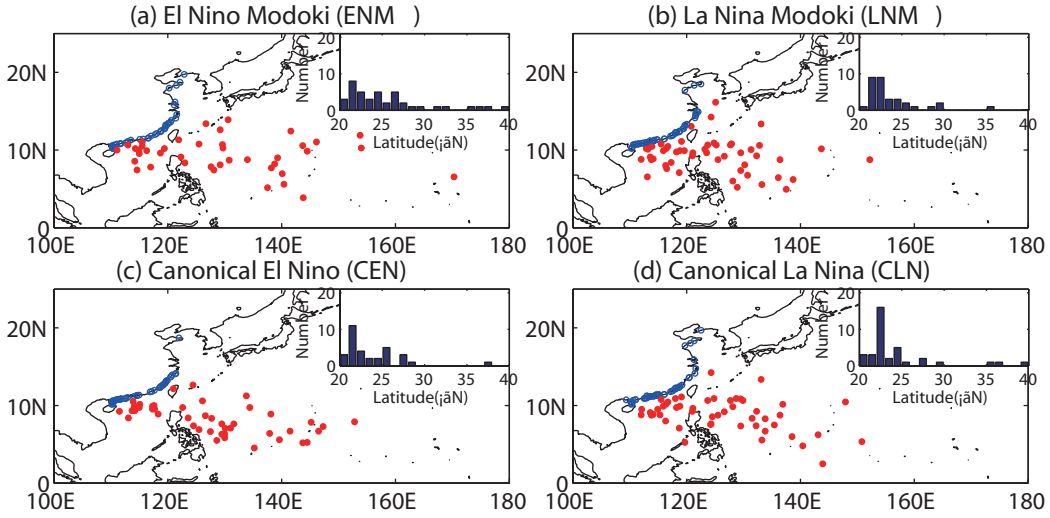

Fig. 2. Genesis points (solid dots), landfall locations (hollow circles) and landfall frequency in unit latitude (histogram) of landfalling TCs in (a) ENM, (b) LNM, (c) CEN and (d) CLN. No genesis point is covered by the histogram in each panel.

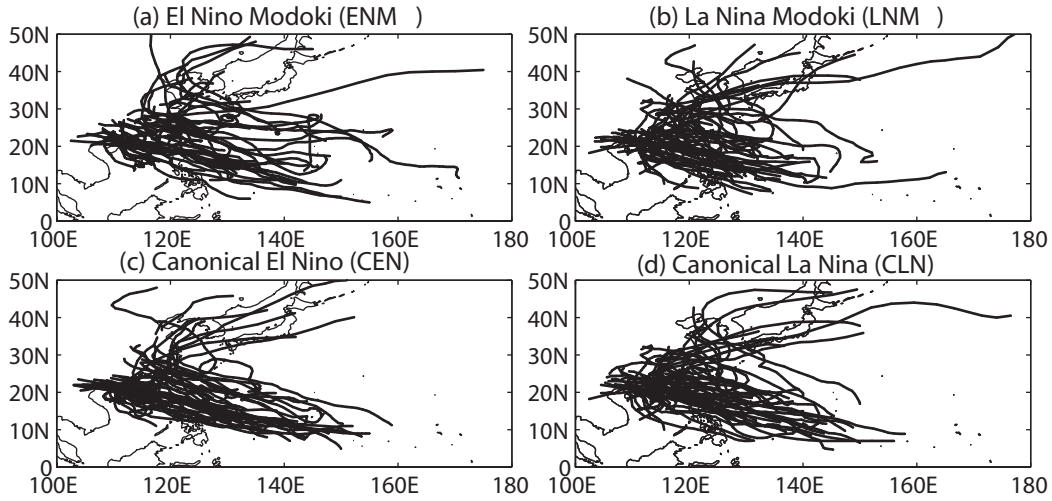

Fig. 3. Tracks (lines) and six-hourly positions (dots) of landfalling TCs in (a) ENM, (b) LNM, (c) CEN and (d) CLN.

the two-tailed *t*-test also shows that total and before-landfall track length and duration are significantly shorter than average in LNM, which we may associate with western genesis location in LNM.

4.5. *Wind and PDI*

Wind reflects the strength of a TC, and research shows that landfalling TCs can cause strong winds over China (Yang and Lei, 2004). In CMA, ENM (LNM) has the weakest (strongest) landfall wind speed, while LNM (CLN) contains the strongest maximum wind speed. Features of wind in JTWC are different from those in CMA, with ENM (CEN) showing the strongest (weakest) landfall wind speed, while ENM (CLN) has the weakest (strongest) maximum wind speed. However, as CMA data use more wind data (Yang and Lei, 2004) than the other two datasets when TCs are close to the land area of China, the results in CMA may be more credible.

PDI combines duration and wind speed, and reflects the potential destructive ability of a TC. Unlike track length and duration, before-landfall PDI and total PDI are strongest in CLN and weakest in LNM. However, features of after-landfall PDI are not consistent between CMA and JTWC. PDI in ENSO Modoki (ENM and LNM) are weaker than in canonical ENSO (CEN and CLN).

5. Large-scale environment

5.1. *Overview*

Landfall position is determined by TC genesis position and track (Liu and Chan, 2003; Wu et al., 2004; Goh and Chan, 2010). TCs tend to form and develop under conditions such as positive low-level vorticity, weak vertical wind shear and above-average mid-level moisture (Gray, 1968; Gray, 1979; Montgomery and Farrell, 1993). In contrast, TC tracks are mainly controlled by the interaction between large-scale environmental steering flow and the β-drift effect (Chan and Gray, 1982; Fiorino and Elsberry, 1989; Wang et al., 1998), with the latter explaining the poleward and westward deviation of TC tracks from the background flow. The monsoon trough (Ramage, 1974; Lander, 1996; Briegel and Frank, 1997; Ritchie and Holland, 1999) and western Pacific subtropical high (WPSH) (Lau and Li, 1984; Wang and Wu, 1997; Ho et al., 2004; Zhang et al., 2012) also modulate TC generation and track. Although the upper air environment, such as tropical upper-tropospheric troughs (TUTTs), can influence TC development and tracks (Sadler, 1978; Montgomery and Farrell, 1993; Ferreira and Schubert, 1999), the present paper does not consider upper air dynamics. In this section, we analyse the non-upper-air environmental factors mentioned above in turn (Figs. 4 and 5), and then consider the effect of combining their impacts. Although the SST anomaly distribution is the basic and essential difference in ENSO events, the SST anomaly in the cyclogenesis region is not significantly different (< 0.5°C) in the four types of ENSO events (Fig. 1). Some studies have shown that the correlation between SST and TCs generated in the WNP is weak (Chan and Liu, 2004; Emanuel, 2005, 2007); thus, we do not discuss SST in this section.

5.2. *Large-scale environment in different ENSO events*

In this paper the low-level flow anomaly is represented by the 850 hPa wind anomaly (Fig. 4). In ENM, a cyclonic wind anomaly ("+" in Fig. 4) in the subtropical WNP near the East Asia coast encourages TC formation. The reverse is true in LNM and CLN, with the anticyclonic wind anomaly in CLN being less pronounced than LNM. The 850 hPa wind anomaly does not show significant rotation in CEN.

Vertical wind shear is defined here as the difference in zonal wind between 200 and 850 hPa (u200 − u850, see Fig. 4). Positive vertical wind shear is stronger in cold events (LNM and CLN) than warm ones (ENM and CEN) near the central Pacific, and this may push the genesis location farther west in cold years than in warm years. The zone of low vertical wind shear (-5 to 5) in CEN is smaller than in the other

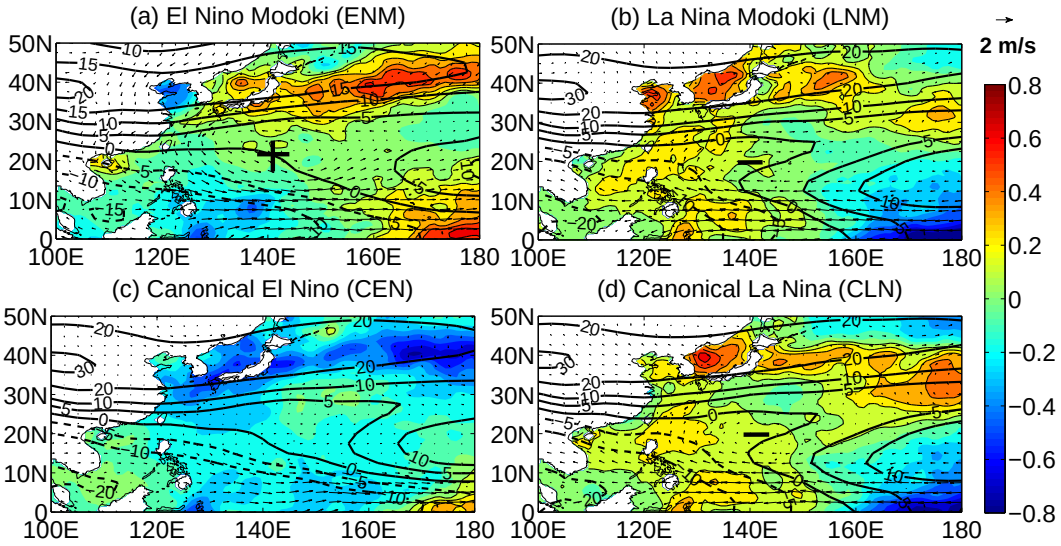

Fig. 4. Composite of JJASO mean SST anomaly (units: °C; shading; positive anomaly in contours), vertical wind shear (u200-u850; bold contours; negative values as dotted lines), and 850 hPa wind anomaly (vectors) in (a) ENM, (b) LNM, (c) CEN and (d) CLN. "+" and "−" signs represent anticyclonic and cyclonic wind anomaly centers, respectively.

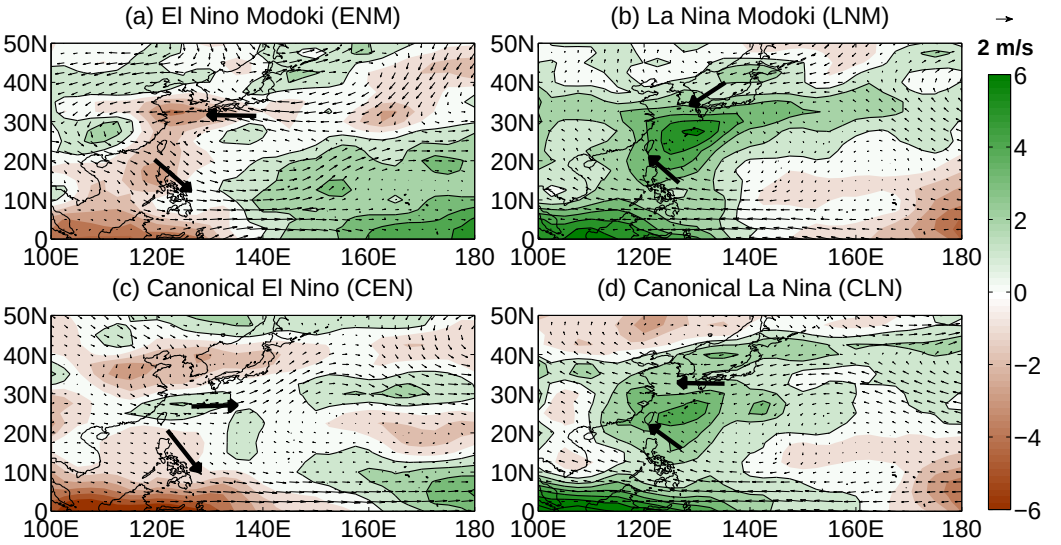

Fig. 5. Composite of JJASO mean 500 hPa relative humidity anomaly (units: %; shading; positive anomaly in contours) and 300–850 hPa mean flow anomaly (arrows) in (a) ENM, (b) LNM, (c) CEN and (d) CLN.

three ENSO events, which suggests a smaller possible TC genesis area in CEN. Note also that the vertical wind shear above 30°N in ENM is about 5 m s^{-1} weaker than in the other three ENSO events, which indicates a weaker destructive effect of vertical wind shear on TCs that try to make landfall above 30°N. If we add the meridional wind, the influence of vertical wind shear does not change (not shown).

Mid-level humidity is represented by the 500 hPa relative humidity (Fig. 5). In ENM, negative (positive) anomalous humidity west (east) of 140°E inhibits (encourages) TC generation, and the reverse is almost the case in LNM and CLN. Unlike ENM, the humidity anomaly in CEN is weak, and seems to weakly modulate TC genesis location to the south.

Mean multilayer steering flow is a better indicator of TC motion than any monolayer flow (Dong, 1983). The strong convergence and divergence in the boundary and outflow layers make it hard to evaluate the vorticity advection correctly (Chan, 1984), and so the rational choice of steering wind is the vertical mean wind between 850 and 300 hPa (Holland, 1984). However, for single stratification, the winds in the mid-troposphere (500–700 hPa) have the strongest correlation with TC movement (Chan and Gray, 1982). The 700, 600 and 500 hPa steering flows (not shown) are very similar to the 300–850 hPa mean (Fig. 5). As the arrows indicate, a northwesterly (easterly) wind anomaly south (north) of 25°N in ENM prevents (guides) TCs from making landfall over the

southern (northern) coastline of China. Northwest and west winds (arrows) in CEN discourage TCs from making landfall along either the southern or the northern track, while the reverse is true in LNM and CLN. Compared with ENM, although the east wind anomaly (arrows above 25°N) in LNM and CLN also encourages TC tracks, the westward-extended WPSH restricts this landfall track. Thus, the TCs prefer to make landfall in a southeastern track.

The monsoon trough and WPSH are closely related (Lau and Li, 1984; Wang and Wu, 1997); they reflect the influence of the environment on TCs from another perspective. The monsoon trough is a preferred (adverse) location for TC genesis, and TCs rarely move into the WPSH. The WPSH is usually represented by the 5880 gpm isoline (Fig. 6). Corresponding to the abnormal northwest (southeast) flow near land between 10°N and 20°N in ENM and CEN (Fig. 5), the monsoon trough extends eastward to about 150°E (127°E) (Fig. 6). In other words, in warm years (ENM and CEN) the monsoon trough extends farther eastward than in cold years (LNM and CLN). The wind speed around the monsoon trough region in ENM is greater than in CEN. The 850 hPa wind field is a good fit to the 850 hPa geopotential height field. Values of geopotential height isolines near the monsoon trough regions are shown in Fig. 6. The 1496 gpm isoline in ENM extends farther east (about 140°E) than in the other three ENSO events (about 127°E), which means that the monsoon trough in the ENM is stronger than in the other three. Related to the monsoon trough, the WPSH in ENM is weaker and smaller in area than in the other three ENSO events, only extending westward to about 150°E. Thus, in ENM the WPSH permits TCs landfalling over China to form and move more to the northeast. Consequently, the monsoon trough in warm years encourages TC genesis farther east than in cold years, and a strong monsoon trough and weak WPSH in ENM seem to produce more and stronger TCs, permitting them to make landfall over more northerly coastlines.

5.3. *Discussion*

Note that because TC tracks in different ENSO events do not show very different patterns (Fig. 3), track length and duration are mainly controlled by genesis location. Tables 3 and 4 also show that southeasterly (northwesterly) genesis locations correspond to longer (shorter) track lengths and durations of landfalling TCs. Therefore, the discussion of environmental factors on TC genesis location also explains the features of track length and duration (especially before-landfall and total ones) to some extent.

Research shows that ENM (LNM) years have double anomalous Walker circulation with common updraft (downdraft) branches near the central Pacific, different from the single cell in CEN (CLN) (Ashok et al., 2007; Ashok and Yamagata, 2009). Circulation modes seem to explain the different environmental factors that affect TCs in different ENSO events: the updraft branch of a double cell in ENM corresponds to weak WNSP. In ENM and CEN (LNM and CLN), sinking flow of anomalous Walker circulation in the WNP is associated with negative (positive) mid-level humidity. Meanwhile, the eastward surface flow of an anomalous Walker cell in ENM and CEN (LNM and CLN) corresponds with a northeasterly (southwesterly) low-level flow anomaly and steering flow anomaly near mainland China under 25°N and a more eastward (westward) extended monsoon trough. Vertical wind shear in LNM and CLN near the central Pacific also seems to be pushed to the west by stronger Walker circulation. These effects of Warlker circulation on the WNP seem to be stronger in ENSO Modoki years (ENM and LNM) than canonical ENSO years (CEN and CLN).

Consequently, we can conclude that TC generation and

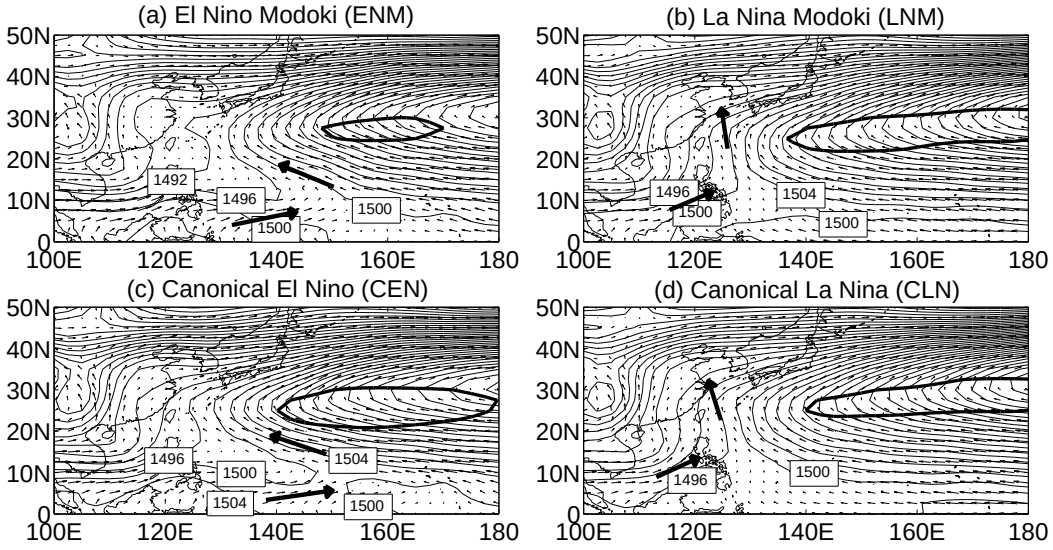

Fig. 6. Composite of JJASO 850 hPa geopotential height (contours; line values near 1500 gpm are shown), 5880 gpm contour at 500 hPa (bold contour) and 850 hPa wind (vectors; bold arrows represent the wind directions around monsoon trough regions) in (a) ENM, (b) LNM, (c) CEN and (d) CLN.

landfall over mainland China are inherently controlled by the internal dynamical processes of the different types of ENSO events.

6. Summary and conclusions

The impact of ENSO Modoki and canonical ENSO on TCs that made landfall over mainland China during 1951–2011 has been analyzed using three TC best-track datasets from China, the USA and Japan. The degree of correlation between characteristic TC quantities and the EMI or Niño3 index were studied first. Following that, TC characteristics in ENM, LNM, CEN and CLN years were identified. Finally, the phenomena of these four types of ENSO events were explained by the effects of environmental factors, including 850 hPa vorticity, vertical wind shear, 500 hPa relative humidity, 300–850 hPa steering flow, the monsoon trough and WPSH.

Higher Niño3 or EMI generally corresponds to higher TC sustainability (track length, duration), but has little significant impact on landfall frequency or TC strength (wind speed, PDI). Although an ENSO effect in moderate years is not obvious, except on sustainability, the effects of each ENSO phase (ENM, LNM, CEN and CLN) are clearer.

Relative to cold phase years (LNM and CLN), landfalling TCs in warm years (ENM and CEN) have a more eastern genesis location, longer track length and duration, both in total and before landfall. Conversely, before-landfall and total destructive ability (PDI) in ENSO Modoki (ENM and LNM) are weaker than in canonical ENSO (CEN and CLN). Each type of ENSO event affects TCs differently.

The impact of ENM is notable, because the atmospheric conditions promote the generation of more TCs over a larger (mainly more northeastern) region, and the steering flow encourages more northerly landfall tracks. ENM has the largest number of TCs that hit mainland China, as well as the most northerly landfall positions and most northeasterly genesis positions; a two-tailed t-test also showed that genesis longitude in ENM is significantly farther east than the 1951–2011 average. ENM also has short after-landfall sustainability (track length and duration). An LSD test showed that landfall latitude may be significantly farther north than in CEN.

The impact of CEN is also interesting because environmental factors modulate TCs so that they are generated farther to the southwest, and the steering flow makes it difficult for TCs to reach mainland China. CEN has low landfall frequency, and the most southerly landfall and genesis locations. The farther southeast genesis location in CEN means that TCs have farther to travel to make landfall, so they have the longest track length and duration. In fact, fewer TCs make landfall to the south in CEN years. LSD results showed that genesis latitude in CEN may be significantly farther south than in ENM or LNM.

The effect of large-scale conditions on landfalling TCs in cold phase years (LNM and CLN) is similar. In LNM and CLN, the anticyclonic wind anomaly and weak monsoon trough inhibit TC generation; the mid-level moisture anomaly, vertical wind shear and WPSH modulate TC generation farther west (west of 140°E), and the steering flow favours TC landfall. This explains why TCs in LNM and CLN have the lowest genesis frequency, moderate landfall and genesis latitude, a more western genesis longitude, and why LNM gives the lowest genesis frequency, and most westerly genesis location. Because of the western genesis location, the tracks and durations of TCs in LNM and CLN are shorter than in ENM and CLN.

Although the large-scale factors considered here partly explain the characteristics of TC frequency, location and sustainability (track length and duration), they do not explain PDI. We also do not know why ENM TCs have short after-landfall track length and duration. Thus, these features are worthy of further study. It may also be useful to examine the intensities of TCs that make landfall over China; for example, distinguishing between weak and strong TCs (typhoons). We have used results averaged over different ENSO events (ENM, CEN, LNM and CLN) in this paper, and closer analysis of a single ENSO year may identify more detailed phenomena. The present study used the Niño-3 index and EMI to define canonical ENSO and ENSO Modoki. This definition may have some shortcomings because 50% of LNM and CLN years overlap, and studies have revealed weaker independence of cold events compared to warm ones. The definition of these four types of ENSO events also requires further study.

Our research has considered the coastline of mainland China and has focused on the dependence of TC landfall on ENSO events in this region. We hope that this research will contribute to our understanding of the impact of different types of ENSO events, and explain some of the variability of TCs that influence China. Because ENSO Modoki has been more frequent and important during recent decades (Ashok et al., 2007; Yeh et al., 2009), the results for ENM and LNM presented in this paper deserve particular attention.

Acknowledgements. This work was supported by The National Natural Science Foundation of China (Grant No. 40976011), the Public Science and Technology Research Funds Projects of Ocean (Grant No. 201105018), and the National Key Basic Research Program of China (Grant No. 2013CB430300).

REFERENCES

Ashok, K., and T. Yamagata, 2009: The El Niño with a difference. *Nature*, **461**, 481–484.

Ashok, K., S. K. Behera, S. A. Rao, H. Weng, and T. Yamagata, 2007: El Niño Modoki and its possible teleconnection. *J. Geophys. Res.*, **112**(C11007), doi: 10.1029/2006jc003798.

Briegel, L. M., and W. M. Frank, 1997: Large-scale influences on tropical cyclogenesis in the western North Pacific. *Mon. Wea. Rev.*, **125**, 1397–1413.

Camargo, S. J., A. W. Robertson, S. J. Gaffney, P. Smyth, and M. Ghil, 2007: Cluster analysis of typhoon tracks. Part II: Large-scale circulation and ENSO. *J. Climate*, **20**(14), 3654–3676, doi: 10.1175/jcli4203.1.

Chan, J. C. L., 1984. Definition of the steering flow for tropical cyclone motion. *15th Conference on Hurricanes and Tropical Meteorology*, Boston, 559–566.

Chan, J. C. L., and W. M. Gray, 1982: Tropical cyclone movement and surrounding flow relationships. *Mon. Wea. Rev.*, **110**, 1354–1374.

Chan, J. C. L., and K. S. Liu, 2004: Global warming and western North Pacific typhoon activity from an observational perspective. *J. Climate*, **17**, 4590–4602.

Chen, G., 2011: How does shifting Pacific ocean warming modulate on tropical cyclone frequency over the South China Sea? *J. Climate*, **24**(17), 4695–4700. doi: 10.1175/2011jcli4140.1.

Chen, G., and C.-Y. Tam, 2010: Different impacts of two kinds of Pacific ocean warming on tropical cyclone frequency over the western North Pacific. *Geophys. Res. Lett.*, **37**(1), doi: 10.1029/2009gl041708.

Chia, H. H., and C. F. Ropelewski, 2002: The interannual variability in the genesis location of tropical cyclones in the northwest Pacific. *J. Climate*, **15**, 2678–2689.

Dong, K., 1983: On the relative motion of binary tropical cyclones. *Mon. Wea. Rev.*, **111**, 945–953.

Elsner, J. B., and K. B. Liu, 2003: Examing the ENSO-typhoon hypothesis. *Climate Research*, **25**, 43–54.

Emanuel, K., 2005: Increasing destructiveness of tropical cyclones over the past 30 years. *Nature*, **436**(7051), 686–688. doi: 10.1038/nature03906.

Emanuel, K., 2007: Environmental factors affecting tropical cyclone power dissipation. *J. Climate*, **20**(22), 5497–5509. doi: 10.1175/2007jcli1571.1.

Ferreira, R. N., and W. H. Schubert, 1999: The role of tropical cyclones in the formation of tropical upper-tropospheric troughs rosana nieto ferreira. *J. Atmos. Sci*., **56**, 2891–2907, doi: 10.1175/1520-0469(1999)056<2891:TROTCI>2.0.CO;2.

Fiorino, M. J., and R. L. Elsberry, 1989: Some aspects of vortex structure related to tropical cyclone motion. *J. Atmos. Sci*., **46**, 975–990.

Fisher, R. A. 1935: *Design of Experiments*. Oliver and Boyd, London, 251 pp.

Fogarty, E. A., J. B. Elsner, T. H. Jagger, K.-B. Liu, and K.-S. Louie, 2006: Variations in typhoon landfalls over China. *Adv. Atmos. Sci*., **23**(5), 665–677, doi: 10.1007/s00376-006-0665-2.

Goh, A. Z.-C., and J. C. L. Chan, 2010: An Improved Statistical Scheme for the Prediction of Tropical Cyclones Making Landfall in South China. *Wea. Forecasting*, **25**, 587–593.

Gray, W. M., 1968: Global view of the origin of tropical disturbances and storms. *Mon. Wea. Rev*., **96**(10), 669–700.

Gray, W. M., 1979: Hurricanes: Their formation, structure and likely role in the general circulation. *Meteorology Over the Tropical Oceans*, D. B. Shaw, Ed., Royal Meteorological Society, 155–218.

Ho, C.-H., J.-J. Baik, J.-H. Kim, D.-Y. Gong, and C.-H. Sui, 2004: Interdecadal changes in summertime typhoon tracks. *J. Climate*, **17**, 1767–1776.

Holland, G. J., 1984: Tropical cyclone motion: A comparison of theory and observation. *J. Atmos. Sci*., **41**(1), 68–75.

Hong, C.-C., Y.-H. Li, T. Li, and M.-Y. Lee, 2011: Impacts of central Pacific and eastern Pacific El Niños on tropical cyclone tracks over the western North Pacific. *Geophys. Res. Lett*., **38**(16), doi: 10.1029/2011gl048821.

Kalnay, E., and Coauthors, 1996: The NCEP/NCAR 40-year reanalysis project. *Bull. Amer. Meteor. Soc.*, **77**(3), 437–471.

Kao, H.-Y., and J.-Y. Yu, 2009: Contrasting Eastern-Pacific and Central-Pacific types of ENSO. *J. Climate*, **22**(3), 615–632. doi: 10.1175/2008JCLI2309.1.

Kim, H.-M., P. J. Webster, and J. A. Curry, 2011: Modulation of north Pacific tropical cyclone activity by three phases of ENSO. *J. Climate*, **24**(6), 1839–1849, doi: 10.1175/2010jcli3939.1.

Kug, J.-S., and Y.-G. Ham, 2011: Are there two types of La Niña? *Geophys. Res. Lett*., **38**(16), doi: 10.1029/2011gl048237.

Kug, J.-S., F.-F. Jin, and S.-I. An, 2009: Two types of El Niño events: Cold tongue El Niño and warm pool El Niño. *J. Climate*, **22**(6), 1499–1515. doi: 10.1175/2008jcli2624.1.

Lander, M. A., 1996: Specific tropical cyclone track types and unusual tropical cyclone motions associated with a reverse-oriented monsoon trough in the western North Pacific. *Wea. Forecasting*, **11**, 170–186, doi: 10.1175/1520-0434(1996)011<0170:STCTTA>2.0.CO;2.

Lau, K.-M., and M. T. Li, 1984: The monsoon of East Asia and its global associations—A survey. *Bull. Amer. Meteor. Soc*., **65**, 114–125.

Liang, J., F. M. Ren, and X. Q. Yang, 2010: Study on the differences between CMA and JTWC tropical cyclone datasets for northwest Pacific. *Acta Oceanologica Sinica*, **32**(1), 10–22. (in Chinese)

Liu, K. S., and J. C. L. Chan, 2003: Climatological characteristics and seasonal forecasting of tropical cyclones making landfall along the south China coast. *Mon. Wea. Rev*., **131**, 1650–1662.

Miller, R. G., Jr., 1966: *Simultaneous Statistical Inference*. McGraw-Hill, New York, 300 pp.

Montgomery, M. T., and B. F. Farrell, 1993: Tropical cyclone formation. *J. Atmos. Sci*., **50**(2), 285–310.

Ramage, C. S., 1974: Monsoonal influences on the annual variation of tropical cyclone development over the indian and Pacific oceans. *Mon. Wea. Rev*., **102**, 745–753.

Rayner, N. A., D. E. Parker, E. B. Horton, C. K. Folland, L. V. Alexander, D. P. Rowell, E. C. Kent, and A. Kaplan, 2003: Global analyses of sea surface temperature, sea ice, and night marine air temperature since the late nineteenth century. *J. Geophys. Res*., **108**(D14), doi: 10.1029/2002jd002670.

Ren, F. M., X. L. Wang, L. S. Chen, and Y. M. Wang, 2008: Tropical cyclones landfalling in the mainland, Hainan and Taiwan of China and their interrelations. *Acta Meteorologica Sinica*, **66**(2), 224–235. (in Chinese)

Ren, F. M., J. Liang, G. X. Wu, W. J. Dong, and X. Q. Yang, 2011: Reliability analysis of climate change of tropical cyclone activity over the western North Pacific. *J. Climate*, **24**(22), 5887–5898. doi: 10.1175/2011jcli3996.1.

Ritchie, E. A., and G. J. Holland, 1999: Large-scale patterns associated with tropical cyclogenesis in the western Pacific. *Mon. Wea. Rev*., **127**, 2027–2043. doi: 10.1175/1520-0493(1999)127<2027:LSPAWT>2.0.CO;2.

Sadler, J. C., 1978: Mid-season typhoon development and intensity changes and the tropical upper tropospheric trough. *Mon. Wea. Rev.*, **106**, 1137–1152.

Wang, B., and R. Wu, 1997: Peculiar temporal structure of the South China Sea summer monsoon. *Adv. Atmos. Sci*., **14**, 177–194.

Wang, B., and J. C. L. Chan, 2002: How strong ENSO events affect tropical strom activity over the western North Pacific. *J. Climate*, **15**, 1643–1658. doi: 10.1175/1520-0442.

Wang, B., R. L. Elsberry, Y. Wang, and L. Wu, 1998: Dynamics

in tropical cyclone motion: A review. *Scientia Atmospherica Sinica*, **22**(4), 535–547.

Wang, S. S., Y. P. Guan, T. Z. Guan, and J. P. Huang, 2012: Oscillation in the frequency of tropical cyclones passing taiwan and hainan islands and the relation with summer monsoon. *Chinese Journal of Oceanology and Limnology*, **30**(6), 966–973, doi: 10.1007/s00343-012-1274-9.

Wang, X.-L., and W.-L. Song, 2009: A study on relationships between ENSO and landfalling tropical cyclones in China. *Journal of Tropical Meteorology*, **25**(5), 576–580. (in Chinese)

Wu, M. C., W. L. Chang, and W. M. Leung, 2004: Impacts of El Niño-Southern Oscillation events on tropical cyclone landfalling activity in the western North Pacific. *J. Climate*, **17**, 1419–1428.

Yang, Y. H., and X. T. Lei, 2004: Statistics of strong wind distribution caused by landfall typhoon in China. *Journal of Tropical Meteorology*, **20**, 633–642. (in Chinese)

Yeh, S.-W., J.-S. Kug, B. Dewitte, M.-H. Kwon, B. P. Kirtman, and F.-F. Jin, 2009: El Niño in a changing climate. *Nature*, **461**(7263), 511–514, doi: 10.1038/nature08316.

Zhang, H., and Y. P. Guan, 2012a: Relationship between the South China Sea summer monsoon and the first-landfall tropical cyclone over mainland of China. *Acta Physica Sinica*, **61**(12), 607–612 . (in Chinese)

Zhang, H., and Y. P. Guan, 2012b: Latitudinal distribution of landing tropical cyclones over mainland China. *Acta Physica Sinica*, **61**(16), 528–534. (in Chinese)

Zhang, W., H.-F. Graf, Y. Leung, and M. Herzog, 2012: Different El Niño types and tropical cyclone landfall in east Asia. *J. Climate*, **25**, 6510–6523, doi: 10.1175/JCLI-D-11-00488.1.